Analysis of $H_{c2}(\theta, T)$ for $Mg(B_{1-x}C_x)_2$ single crystals by using the dirty two-gap model

2007 J. Phys.: Condens. Matter 19 242201

(http://iopscience.iop.org/0953-8984/19/24/242201)

IOP FTC

IOP PUBLISHING JOURNAL OF PHYSICS: CONDENSED MATTER

J. Phys.: Condens. Matter **19** (2007) 242201 (7pp) doi:10.1088/0953-8984/19/24/242201

FAST TRACK COMMUNICATION

Analysis of $H_{c2}(\theta, T)$ for $Mg(B_{1-x}C_x)_2$ single crystals by using the dirty two-gap model

Min-Seok Park[1], Hyun-Sook Lee[1], Jung-Dae Kim[1], Heon-Jung Kim[1], Myung-Hwa Jung[2], Younghun Jo[2] and Sung-Ik Lee[1]

[1] National Creative Research Initiative Center for Superconductivity and Department of Physics, Pohang University of Science and Technology, Pohang 790-784, Republic of Korea
[2] Quantum Material Laboratory, Korea Basic Science Institute, Daejeon 305-333, Republic of Korea

E-mail: silee@postech.ac.kr

Received 1 May 2007
Published 18 May 2007
Online at stacks.iop.org/JPhysCM/19/242201

Abstract

To understand the effect of carbon doping on the superconductivity in MgB_2, we obtained the angle- and temperature-dependent upper critical fields [$H_{c2}(\theta)$ and $H_{c2}(T)$] for $Mg(B_{1-x}C_x)_2$ single crystals ($x = 0.06$ and 0.1) from resistivity measurements while varying the temperature, the field, and the direction of the field. The detailed values of the diffusivity for two different directions for each σ-band and π-band were obtained to explain both the temperature- and the angle-dependent H_{c2} by using the dirty-limit two-gap model. The induced impurity scattering of the σ-band and the π-band for both the ab-plane and the c-direction is studied.

1. Introduction

Soon after the discovery of superconductivity in MgB_2 [1], two-gap superconductivity was discovered [2–4]. Although this two-gap nature has been established by tunnelling [5–7], heat capacity [8], Raman [9], point contact spectroscopy [10, 11], and reversible magnetization measurements [12, 13], understanding how the two-gap nature of superconductivity evolves with selective doping is also important. Among various atoms, only carbon (C) for boron (B) [14] and aluminium (Al) for magnesium (Mg) [15] have been successfully doped. While the two superconducting gaps of $(Mg_{1-x}Al_x)B_2$ survive for $x = 0.21$ [16], the two gaps of $Mg(B_{1-x}C_x)_2$ are preserved only for $x < 0.132$ [17].

Why are the two distinct gaps preserved up to high doping concentrations? It is believed that interband scattering mixes two different bands, thus leading to gap merging. However, as argued by Mazin *et al* [18], σ–π interband impurity scattering is small because of the orthogonality between the two orbitals. Erwin and Mazin [19] went a step further and predicted a method to mix these two bands. When Na and Al are co-doped on the Mg site in MgB_2,

an out-of-plane distortion is induced, and the two bands are mixed; thus, the two gaps will eventually merge into one gap. In this case, the band-filling effect is compensated for by the opposing trends of Na and Al, so the interband scattering effect is more effective. Most doping in the B-plane does not induce out-of-plane distortion, so σ–π interband scattering is not induced. However, Samuely *et al* [20] argued that the band-filling effect was sufficient, so interband scattering was not needed to explain the decreasing two-gap superconductivity, which was in opposition to the explanation of interband scattering by Gonnelli *et al* [17]. The relationship between interband scattering and the C concentration is still controversial.

Even several years after the discovery of superconductivity in this material, the angle and the magnetic field dependences of transport for carbon-doped MgB_2 have not been studied in detail. These dependences of H_{c2} will give valuable information, such as the directional diffusivity of each of the two bands and interband scattering and thus the development of the two-gap superconductivity.

In this letter, we present the $H_{c2}(T, \theta)$ obtained from transport measurements for $Mg(B_{1-x}C_x)_2$ single crystals ($x = 0.06$ and 0.1). The temperature and the angle dependences of the H_{c2} are analysed on the basis of the dirty-limit two-gap model (TGM). The obtained diffusivities ($D^{ab,c}_{\sigma,\pi}$) indicate that in-plane impurity scattering in the σ-band and out-of-plane impurity scattering in the π-band are quite enhanced with C doping. Also, $Mg(B_{1-x}C_x)_2$ for $x = 0.06$ and 0.1 turns out to be in the region of the dirty σ-band. We also find that C substitution influences interband scattering in MgB_2 much more effectively than Al substitution does [16].

2. Experiment

The single crystals for this study were synthesized under high-pressure and high-temperature conditions. A mixture of $Mg{:}B_{1-x}C_x = 1{:}1$ with Mg (99.6%, 200-mesh, Alfa Aesar), amorphous B (99.99%, 325-mesh, Alfa Aesar), and B_4C (200-mesh, Aldrich) powders was ground in a glove box filled with inert Ar gas. The resulting precursor was pelletized, wrapped in a BN sleeve, and put into a high-pressure cubic cell. The cell was pressed up to 3 GPa and heated at 1450 °C for 1 h. The temperature was then gradually decreased to about 900 °C over 5 h. Figure 1(a) shows the four-probed $Mg(B_{0.9}C_{0.1})_2$ single crystal made by using photolithography. Four-probe contacts using photolithography are possible because of the single crystals being long and thin, with clean and shiny surfaces. However, only one out of a few hundred single crystals has these characteristics.

The relationship between T_c suppression and C concentration is consistent with previously reported relationships based on neutron diffraction [21], Auger electron spectroscopy [22], and x-ray diffraction [14, 22–26]. The low-field magnetization, $M(T)$, was measured using a superconducting quantum interference device (MPMSXL, Quantum Design). Four probes were successfully contacted by using photolithographic techniques [27]. The selected single crystals were $\sim 200 \times 20 \times 15\ \mu m^3$. The temperature- and angle-dependent resistivities $R(T, \theta)$ were obtained for magnetic fields up to 9 T.

3. Results and discussion

Figure 1(b) is the resistivity $\rho(T)$ for $Mg(B_{1-x}C_x)_2$ with $x = 0$, 0.06 and 0.1. The T_cs, which decrease as carbon doping is increased, are 37 K, 32 K, and 26 K for $x = 0$, 0.06, and 0.1, respectively. The resistive transitions with $\delta T_c(0\text{–}100\%) \leqslant 0.5$ K are very sharp, which implies that the quality of these samples is very high. In figure 1(b), the Bloch–Grüneisen (BG) formula [27], which contains the electron–phonon interaction but not the

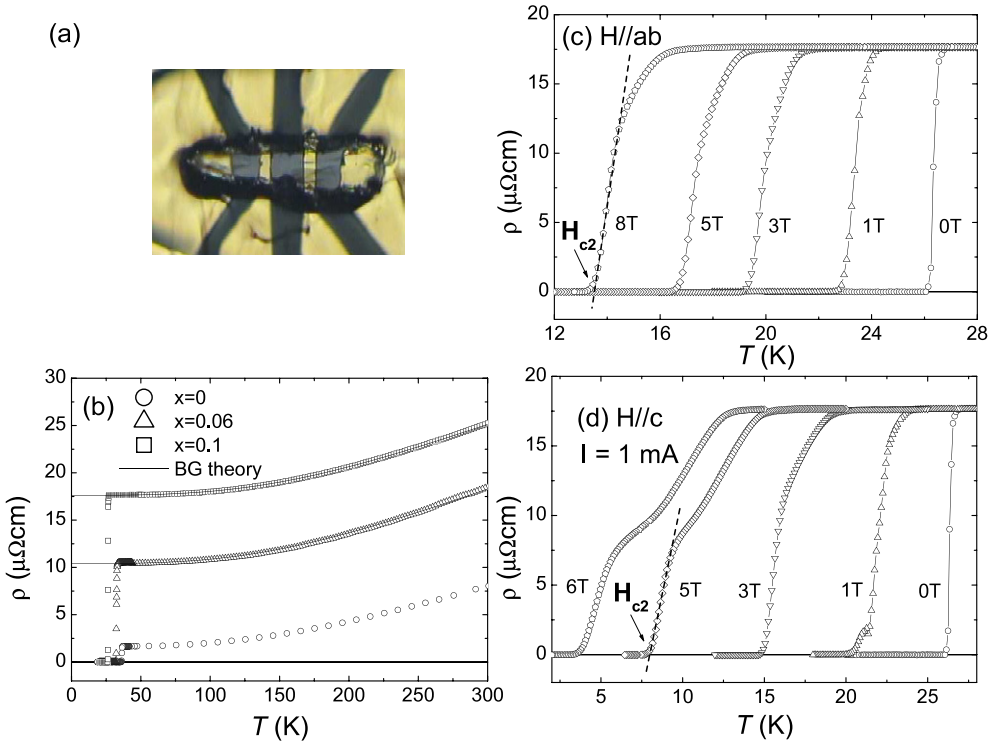

Figure 1. (a) The inset shows the four probes of a $Mg(B_{0.9}C_{0.1})_2$ single crystal. The probes were formed by using photolithography. (b) Temperature-dependent resistivities $\rho(T)$ of $Mg(B_{1-x}C_x)_2$ for $x = 0$ (circles), 0.06 (triangles), and 0.1 (squares). The solid lines indicate the Bloch–Grüneisen fitting. Temperature-dependent resistivities $\rho(T, H)$ of $Mg(B_{0.9}C_{0.1})_2$ for magnetic fields (c) parallel to the ab-plane and (d) parallel to the c-axis.

(This figure is in colour only in the electronic version)

electron–electron interaction, is used to describe the normal-state resistivity for $Mg(B_{1-x}C_x)_2$. The Debye temperature Θ_D and the residual resistivity ρ_0 are 1170 K (1220 K) and 10.4 $\mu\Omega$ cm (17.6 $\mu\Omega$ cm), respectively, for $x = 0.06$ (0.1). These Θ_D s are slightly larger than the Θ_D of ∼1100 K for pure MgB_2 single crystals [27]. The ρ_0, which increases by several times with C doping, indicates that impurity scattering is not small.

Figures 1(c) and (d) are the $\rho(T)$ for $x = 0.1$ for $H \parallel ab$ and $H \parallel c$, respectively. From the figures, we immediately notice the two different resistive transitions with different origins. Actually, the transition at higher temperature originates from the surface superconductivity and the lower transition is from the bulk transition. In detail, as the temperature decreases, $\rho(T)$ decreases slowly and then drops sharply to zero. The former case results from surface superconductivity, which is stronger for $H \parallel c$ than for $H \parallel ab$. Similar phenomena were observed in pristine [28] and Al-doped [16] MgB_2 single crystal. The latter transition is a bulk transition. $H_{c2}^{ab,c}(T)$ is determined as the crossover point between the sharp resistive drop line and the $\rho = 0$ line, as indicated by the arrows in figures 1(c) and (d).

For a more quantitative analysis, the TGM [29, 30] is adopted. This model predicts both the angle and temperature dependences of H_{c2} simultaneously, so the physical quantities should be determined most accurately. So far, simultaneous measurements of the angle and temperature dependences of H_{c2} for C-doped MgB_2 have not been reported. Since we can obtain H_{c2} for

Table 1. T_c is the transition temperature. The diffusivities [$D_\sigma^{ab,c}$ and $D_\pi^{ab,c}$] in the σ- and π-bands in the ab-plane and along the c-axis are obtained from fitting $H_{c2}(\theta)$ by using the dirty-limit two-gap model. Since MgB_2 is believed to exist in the clean limit [34–36], data for $x = 0$ are not included.

x	T_c (K)	D_σ^{ab} ($m^2\ s^{-1}$)	D_σ^{c} ($m^2\ s^{-1}$)	D_π^{ab} ($m^2\ s^{-1}$)	D_π^{c} ($m^2\ s^{-1}$)
0.06	32	3.7×10^{-4}	6×10^{-5}	3.4×10^{-2}	4.4×10^{-1}
0.1	26	2.4×10^{-4}	6.6×10^{-5}	6×10^{-2}	1.5×10^{-1}

both variables, the analysis of the TGM should be much better than the measurement of the temperature only. In this sense, we obtain much more information, such as the diffusivities, $D_{\sigma,\pi}$, for the σ- and π-bands separately.

We briefly introduce the TGM developed by Gurevich and Koshelev *et al* [29, 30]. In this theory, the Usadel equations for an anisotropic two-gap superconductor were derived from the general Eilenberger equation [31]. From these equations, the upper critical field for a two-gap superconductor can be obtained. In the absence of interband scattering, $H_{c2}(T)$ for $H \parallel c$ ($\theta = 0°$) is

$$a_0 [\ln t + U(h)] [\ln t + U(\eta h)] + a_2 [\ln t + U(\eta h)] + a_1 [\ln t + U(h)] = 0, \tag{1}$$

where $t = \frac{T}{T_c}$, $h = \frac{H_{c2} D_\sigma^{ab}}{2\phi_0 T}$, $\eta = \frac{D_\pi^{ab}}{D_\sigma^{ab}}$, $U(x) = \psi(\frac{1}{2} + x) - \psi(x)$, and $a_{0,1,2}$ are constants derived from the electron–phonon coupling constants (λ_{mn}^{ep}) and the Coulomb pseudopotentials (μ_{mn}) for each doping level [32]. ϕ_0, $D_{\sigma,\pi}^{ab}$, and $\psi(x)$ represent the magnetic flux quantum, the in-plane electron diffusivities in the σ- and π-bands, and the di-gamma function, respectively. For the isotropic case, $D = \frac{l v_F^2}{3}$, where l is the mean free path and v_F is the Fermi velocity. For $H \parallel ab$ ($\theta = 90°$), $D_{\sigma,\pi}^{ab}$ is replaced by $(D_{\sigma,\pi}^{ab} D_{\sigma,\pi}^{c})^{\frac{1}{2}}$, where $D_{\sigma,\pi}^{c}$ is the out-of-plane electron diffusivity. In order to investigate the angular dependence of H_{c2}, equation (1) is generalized to the anisotropy case by substituting $D_{\sigma,\pi}(\theta) = [(D_{\sigma,\pi}^{ab})^2 \cos^2\theta + D_{\sigma,\pi}^{ab} D_{\sigma,\pi}^{c} \sin^2\theta]^{\frac{1}{2}}$ for $D_{\sigma,\pi}^{ab,c}$. Equation (1) and $D_{\sigma,\pi}(\theta)$ give the following angular dependence of H_{c2} near T_c:

$$H_{c2}(\theta) \frac{8\phi_0 (T_c - T)}{\pi^2 [a_1 D_\sigma(\theta) + a_2 D_\pi(\theta)]}. \tag{2}$$

For $D_\sigma = D_\pi$, equation (2) becomes the well-known anisotropic one-gap Ginzburg–Landau model (OGM), and $H_{c2} = \frac{4\phi_0 (T_c - T)}{\pi^2 D(\theta)}$ for a dirty one-gap superconductor. However, for $D_\sigma \neq D_\pi$, the angle-dependent H_{c2} equation ends in deviations of $H_{c2}(\theta)$ for OGM; $H_{c2}(\theta) = H_{c2}^{ab}(0)(\sqrt{\cos^2\theta + \gamma^2 \sin^2\theta})^{-1}$, where γ is the anisotropy ratio of $H_{c2}(\theta = 90°)$ to $H_{c2}(\theta = 0°)$. The details are described in an earlier publication [29].

Figure 2(a) shows the $H_{c2}(\theta)$ for $x = 0.06$ and 0.1, obtained from the field-dependent resistivity $\rho(H)$ at various angles. The H_{c2} data for $\theta = 90°$ are omitted because the strong surface superconductivity screens the real H_{c2} at this angle. To determine $H_{c2}(\theta)$, we apply our data to the TGM first and then to the OGM later. The solid lines in figure 2(a) are the theoretical curves calculated using the TGM, while the dotted lines are calculated using the OGM. The TGM reproduces the experimental data better than the OGM for $x = 0.06$, but the difference between the two is quite small. The OGM near $\theta = 0°$ deviates slightly from the experimental data.

In the above analysis, we find that the calculated D_σ is much smaller than D_π for both directions (see table 1), which means that C doping induces the σ-band in the dirty limit. One also expects that, once B is replaced by C, in-plane impurity scattering in the σ-band and out-of-plane impurity scattering in the π-band will definitely be enhanced. This is confirmed by the experimental analysis; D_σ^{ab} and D_π^{c} decrease systematically with increasing C doping. The

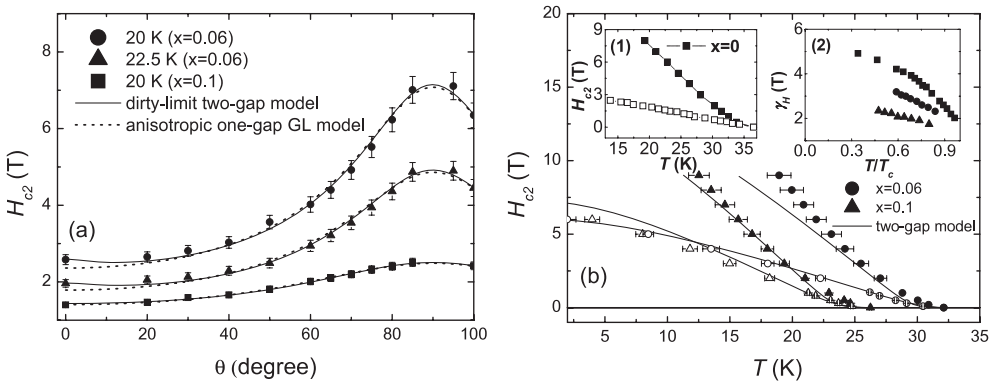

Figure 2. (a) The solid symbols show the angle-dependent upper critical field $H_{c2}(\theta)$. The error bar obtained from the transition width is below 5%. The solid lines are obtained from the dirty-limit two-gap model, while the dotted lines are obtained from the one-gap Ginzburg–Landau model. (b) The upper critical fields $H_{c2}(T)$ versus temperature. The solid symbols are H_{c2} for $H \parallel ab$, whereas the hollow symbols are H_{c2} for $H \parallel c$. For comparison, the temperature dependence of $H_{c2}(T)$ for $x = 0$ is shown in inset (1). Inset (2) shows the temperature dependence of the upper critical anisotropy, $\gamma_H(T)(=H_{c2}^{ab}(T)/H_{c2}^{c}(T))$, for $x = 0$ (squares), 0.06 (circles), and 0.1 (triangles).

D_σ^c is already very small compared to the D_σ^{ab}. Also, the D_π^{ab} is quite small compared to the D_π^c for this composition.

In figure 2(b), the $H_{c2}^{ab,c}(T)$ is shown. Circles are for $x = 0.06$ and triangles are for $x = 0.1$. Solid symbols show $H_{c2}(T)$ for $H \parallel ab$, while hollow symbols show $H_{c2}(T)$ for $H \parallel c$. The maximum error originating from the transition width at high fields is about 5%. For comparison, the $H_{c2}^{ab,c}(T)$ for pure MgB_2 is plotted in inset (1) of figure 2(b). It is interesting to notice that the $H_{c2}(T)$ near T_c shows an almost linear pattern for $x = 0$, while $H_{c2}(T)$ near T_c show a distinct upward curvature for $x = 0.06$ and 0.1.

The inset (2) of figure 2(b) shows $\gamma_H(T)$. As C increases, γ_H decreases, but still shows a strong temperature dependence even for $x = 0.1$. The range of γ_H is about 1.5–2 near T_c. The decreasing behaviour of γ_H has been observed previously [24, 33]. According to the TGM, $\gamma_H(T)$ in the dirty σ-band region decreases with increasing T, whereas $\gamma_H(T)$ in the dirty π-band region increases with increasing T. In contrast, $\gamma_H(T)$ within the OGM is temperature independent and is a simple constant. Thus, the temperature dependence of $\gamma_H(T)$ derived from $H_{c2}^{ab,c}(T)$ can be explained by using the TGM.

How do we explain the distinct upward curvature of $H_{c2}(T)$ near T_c for $x = 0.06$ and 0.1 and the linear behaviour for $x = 0$? According to the TGM, if the π-band is dirtier than the σ-band, $H_{c2}(T)$ is linear near T_c; on the other hand, if the σ-band is dirtier than the π-band, $H_{c2}(T)$ shows an upward curvature near T_c. In fact, C doping induces the σ-band to become quite dirty. This is confirmed by the D obtained from the TGM, as shown in table 1.

We analyse the experimental data of $H_{c2}(T)$ with $D_{\sigma,\pi}^{ab,c}$, while comparing it with the TGM by fitting $H_{c2}(\theta)$, as shown in table 1 and figure 2(b). The solid lines are the curves calculated from the TGM. Within the error bars, the curves can reproduce $H_{c2}^{c}(T)$ for $x = 0.06$ and $H_{c2}^{ab}(T)$ for $x = 0.1$. $H_{c2}^{ab}(T)$ for $x = 0.06$ is slightly underestimated for $H > 5$ T, while $H_{c2}^{c}(T)$ for $x = 0.1$ is slightly overestimated for $H > 4$ T. Note that the upward curvature of $H_{c2}(T)$ near T_c can be described well by using the TGM.

We have described both the angle and temperature dependences of H_{c2} for $Mg(B_{1-x}C_x)_2$ ($x = 0.06$ and 0.1) by using the TGM and have thus proven that our samples are in the

dirty σ-band region. Moreover, the σ-band in the ab-plane and the π-band along the c-axis become notably dirty from $x = 0.06$ to 0.1. The temperature-dependent $\gamma_H(T)$ and the upward curvature of $H_{c2}(T)$ near T_c are well described using the TGM. However, compared to $H_{c2}(\theta)$ for the Al-doped case [16], interband scattering, and thus the tendency to one-gap superconductivity, in C-doped MgB_2 may be stronger.

4. Conclusions

We present the $H_{c2}(T, \theta)$ obtained from transport measurements for $Mg(B_{1-x}C_x)_2$ single crystals ($x = 0.06$ and 0.1). Both the temperature and the angle dependences of H_{c2} are well described by the dirty-limit two-gap model. The diffusivity of the σ-band is quite small compared to that of the π-band, which indicates that C-doped MgB_2 is in the dirty σ-band region. The obtained diffusivity ($D^{ab,c}_{\sigma,\pi}$) indicates that in-plane impurity scattering in the σ-band and out-of-plane impurity scattering in the π-band increase with increasing C doping. The difference between the values of $H_{c2}(\theta)$ obtained by using both the one-gap Ginzburg–Landau model and the dirty two-gap model is smaller than that obtained for Al-doped single crystals [16]. This indicates that C substitution in MgB_2 influences the interband scattering more than Al substitution does.

Acknowledgements

This work is supported by the Ministry of Science and Technology of Korea through the Creative Research Initiative Program. This work is partially supported by the Korea Research Council of Fundamental Science & Technology (KRCF).

References

[1] Nagamatsu J, Nakagawa N, Muranaka T, Zenitani Y and Akimitsu J 2001 *Nature* **410** 63
[2] Kortus J, Mazin I I, Belashchenko K D, Antropov V P and Boyer L L 2001 *Phys. Rev. Lett.* **86** 4656
[3] Choi H J, Roundy D, Sun H, Cohen M L and Louie S G 2002 *Nature* **418** 758
[4] Souma S *et al* 2001 *Nature* **423** 65
[5] Giubileo F, Roditchev D, Sacks W, Lamy R, Thanh D X, Klein J, Miraglia S, Fruchart D, Marcus J and Monod Ph 2001 *Phys. Rev. Lett.* **87** 177008
[6] Iavarone M *et al* 2002 *Phys. Rev. Lett.* **89** 187002
[7] Schmidt H, Zasadzinski J F, Gray K E and Hinks D G 2002 *Phys. Rev. Lett.* **88** 127002
[8] Bouquet F, Fisher R A, Phillips N E, Hinks D G and Jorgensen J D 2001 *Phys. Rev. Lett.* **87** 047001
[9] Chen X K, Konstantinovic M J, Irwin J C, Lawrie D D and Franck J P 2001 *Phys. Rev. Lett.* **87** 157002
[10] Szabo P, Samuely P, Kacmarcik J, Klein T, Marcus J, Fruchart D, Miraglia S, Marcenat C and Jansen A G M 2001 *Phys. Rev. Lett.* **87** 137005
[11] Gonnelli R S, Daghero D, Ummarino G A, Stepanov V A, Jun J, Kazakov S M and Karpinski J 2002 *Phys. Rev. Lett.* **89** 247004
[12] Kang B, Kim H-J, Park M-S, Kim K-H and Lee S-I 2004 *Phys. Rev.* B **69** 144514
[13] Kim H-J, Kang B, Park M-S, Kim K-H, Lee H-S and Lee S-I 2004 *Phys. Rev.* B **69** 184514
[14] Takenobu T, Ito T, Chi D H, Prassides K and Iwasa Y 2001 *Phys. Rev.* B **64** 134513
[15] Slusky J S *et al* 2001 *Nature* **410** 343
[16] Kim H-J, Lee H S, Kang B, Yim W-H, Jo Y, Jung M-H and Lee S-I 2006 *Phys. Rev.* B **73** 064520
[17] Gonnelli R S, Daghero D, Calzolari A, Ummarino G A, Dellarocca V, Stepanov V A, Kazakov S M, Zhigadlo N and Karpinski J 2005 *Phys. Rev.* B **71** 060503(R)
[18] Mazin I I, Andersen O K, Jepsen O, Dolgov O V, Kortus J, Golubov A A, Kuz'menko A B and van der Marel D 2002 *Phys. Rev. Lett.* **89** 107002
[19] Erwin S C and Mazin I I 2003 *Phys. Rev.* B **68** 132505
[20] Samuely P, Szabo P, Canfield P C and Bud'ko S L 2005 *Phys. Rev. Lett.* **95** 099701
[21] Avdeev M, Jorgensen J D, Ribeiro R A, Bud'ko S L and Canfield P C 2003 *Physica* C **387** 301

[22] Lee S, Masui T, Yamamoto A, Uchiyama H and Kajima S 2003 *Physica* C **397** 7
[23] Wilke R H T, Bud'ko S L, Canfield P C, Finnemore D K, Suplinskas R J and Hannahs S T 2004 *Phys. Rev. Lett.* **92** 217003
[24] Kazakov S M, Puzniak R, Rogacki K, Mironov A V, Zhigadlo N D, Jun J, Soltmann Ch, Batlogg B and Karpinski J 2005 *Phys. Rev.* B **71** 024533
[25] Ribeiro R A, Bud'ko S L, Petrovic C and Canfield P C 2003 *Physica* C **384** 227
[26] Mickelson W, Cumings J, Han W Q and Zettl A 2002 *Phys. Rev.* B **65** 052505
[27] Kim Kijoon H P *et al* 2002 *Phys. Rev.* B **65** 100510(R)
[28] Rydh A *et al* 2003 *Phys. Rev.* B **68** 172502
[29] Gurevich A 2003 *Phys. Rev.* B **67** 184515
[30] Koshelev A E and Golubov A A 2003 *Phys. Rev. Lett.* **90** 177002
[31] Eilenberger G 1969 *Z. Phys.* **214** 195
Larkin A I and Ovchinnikov Yu N 1968 *Zh. Exp. Teor. Fiz.* **55** 2262
Larkin A I and Ovchinnikov Yu N 1969 *Sov. Phys.—JETP* **28** 1200
[32] Ummarino G A, Daghero D, Gonnelli R S and Moudden A H 2005 *Phys. Rev.* B **71** 134511
[33] Krutzler C, Zehetmayer M, Eisterer M, Weber H W, Zhigadlo N D, Karpinski J and Wisniewski A 2006 *Phys. Rev.* B **74** 144511
[34] Yelland E A, Cooper J R, Carrington A, Hussey N E, Meeson P J, Lee S, Yamamoto A and Tajima S 2002 *Phys. Rev. Lett.* **88** 217002
[35] Eskildsen M R, Kugler M, Tanaka S, Jun J, Kazakov S M, Karpinski J and Fischer Ø 2002 *Phys. Rev. Lett.* **89** 187003
[36] Quilty J W, Lee S, Tajima S and Yamanaka A 2003 *Phys. Rev. Lett.* **90** 207006